The Lick-Carnegie Exoplanet Survey: A 3.1 $M_\oplus$ Planet in the Habitable Zone of the Nearby M3V Star Gliese 581

Steven S. Vogt[1], R. Paul Butler[2], E. J. Rivera[1], N. Haghighipour[3], Gregory W. Henry[4], and Michael H. Williamson[4]

Received _____; accepted _____

ms-press

[1]UCO/Lick Observatory, University of California, Santa Cruz, CA 95064

[2]Department of Terrestrial Magnetism, Carnegie Institution of Washington, 5241 Broad Branch Road, NW, Washington, DC 20015-1305

[3]Institute for Astronomy and NASA Astrobiology Institute, University of Hawaii-Manoa, Honolulu, HI 96822

[4]Tennessee State University, Center of Excellence in Information Systems, 3500 John A. Merritt Blvd., Box 9501, Nashville, TN. 37209-1561

ABSTRACT

We present 11 years of HIRES precision radial velocities (RV) of the nearby M3V star Gliese 581, combining our data set of 122 precision RVs with an existing published 4.3-year set of 119 HARPS precision RVs. The velocity set now indicates 6 companions in Keplerian motion around this star. Differential photometry indicates a likely stellar rotation period of $\sim$ 94 days and reveals no significant periodic variability at any of the Keplerian periods, supporting planetary orbital motion as the cause of all the radial velocity variations. The combined data set strongly confirms the 5.37-day, 12.9-day, 3.15-day, and 67-day planets previously announced by Bonfils et al. (2005), Udry et al. (2007), and Mayor et al. (2009). The observations also indicate a 5th planet in the system, GJ 581f, a minimum-mass 7.0 $M_{\oplus}$ planet orbiting in a 0.758 AU orbit of period 433 days and a 6th planet, GJ 581g, a minimum-mass 3.1 $M_{\oplus}$ planet orbiting at 0.146 AU with a period of 36.6 days. The estimated equilibrium temperature of GJ 581g is 228 K, placing it squarely in the middle of the habitable zone of the star and offering a very compelling case for a potentially habitable planet around a very nearby star. That a system harboring a potentially habitable planet has been found this nearby, and this soon in the relatively early history of precision RV surveys, indicates that $\eta_{\oplus}$, the fraction of stars with potentially habitable planets, is likely to be substantial. This detection, coupled with statistics of the incompleteness of present-day precision RV surveys for volume-limited samples of stars in the immediate solar neighborhood suggests that $\eta_{\oplus}$ could well be on the order of a few tens of percent. If the local stellar neighborhood is a representative sample of the galaxy as a whole, our Milky Way could be teeming with potentially habitable planets.

Subject headings: stars: individual: GJ 581 HIP 74995 – stars: planetary systems – astrobiology

1. Introduction

There are now nearly 500 known extrasolar planets, and discovery work continues apace on many fronts: by radial velocities (RV), gravitational microlensing, transit surveys, coronography, nulling interferometry, and astrometry. By far the most productive discovery technique to date has been through the use of precision RVs to sense the barycentric reflex velocity of the host star induced by unseen orbiting planets. In recent years, the world's leading RV groups have improved precision down to the $\sim$1 ms^{-1} level, and even below, extending detection levels into the range of planets with masses less than $10\,M_{\oplus}$, commonly referred to as "Super-Earths". This level of precision is now bringing within reach one of the holy grails of exoplanet research, the detection of $\sim$Earth-size planets orbiting in the habitable zones (HZ) of stars. Nearby K and M dwarfs offer the best possibility of such detections, as their HZ's are closer in, with HZ orbital periods in the range of weeks to months rather than years. These low mass stars also undergo larger reflex velocities for a given planet mass. To this end, we have had a target list of $\sim$400 nearby quiet K and M dwarfs under precision RV survey with HIRES at Keck for the past decade.

One of these targets, the nearby M3V star GJ 581 (HIP 74995), has received considerable attention in recent years following the announcement by Bonfils et al. (2005), hereafter Bonfils05, of a 5.37-day hot-Neptune (GJ 581b, or simply planet-b) around this star. More recently, the Geneva group (Udry et al. 2007), hereafter Udry07, announced the detection of two additional planets (c and -d) in this system, one close to the inner edge of the HZ of this star and the other close to the outer edge. Planet-c was reported to have a period of 12.931 days and $m \sin i = 5.06\,M_{\oplus}$ whereas planet-d was reported to have a period of 83.4 days and $m \sin i = 8.3\,M_{\oplus}$.

The Geneva group's announcement of planet-c generated considerable excitement because of its small minimum mass ($5\,M_{\oplus}$, well below the masses of the ice giants of

our solar system and potentially in the regime of rocky planets or Super-Earths) and its location near the inner edge of the HZ of this star. An assumed Bond albedo of 0.5 yielded a simple estimate of ∼320 K for the equilibrium temperature of the planet, suggesting the possibility that it was a habitable Super-Earth. However, a more detailed analysis by Selsis et al. (2007), that included the greenhouse effect and the spectral energy distribution of GJ 581, concluded that planet-c's surface temperature is much higher than the equilibrium temperature calculated by Udry07 and that it is unlikely to host liquid water on its surface. Selsis et al. (2007) concluded that both planets c and d are demonstrably outside the conservative HZ of this star, but that given a large atmosphere, planet-d could harbor surface liquid water. Chylek & Perez (2007) reached a similar conclusion that neither planets c nor d is in the HZ, but that planet-d could achieve habitability provided a greenhouse effect of 100 K developed. Moreover, if these planets are tidally spin-synchronized, planet-c could conceivably have atmospheric circulation patterns that might support conditions of habitability. von Bloh et al. (2007) also concluded that planet-c is too close to the star for habitability. They argue, however, that if planet-d has a thick atmosphere and is tidally locked, it may lie just within the outer edge of the HZ. Both von Bloh et al. (2007) and Selsis et al. (2007) conclude that planet-d would be an interesting target for the planned TPF/Darwin missions.

Beust et al. (2008) studied the dynamical stability and evolution of the GJ 581 system using the orbital elements of Udry07, which they integrated forward for 10^8 years. They observed bounded chaos (see e.g. Laskar (1997)), with small-amplitude eccentricity variations and stable semi-major axes. Their conclusions were unaffected by the presence of any as-yet-undetected outer planets. On dynamical stability grounds, they were able to exclude inclinations $i \leq 10^\circ$ (where $i = 0^\circ$ is face-on).

Last year, Mayor et al. (2009), hereafter Mayor09, published a velocity update wherein

they revised their previous claim of an 8 $M_\oplus$ planet orbiting with an 83-day period, to a 7.1 $M_\oplus$ planet orbiting at 67-days, citing confusion with aliasing for the former incorrect period. Mayor09 also reported another planet in the system at 3.148 days with a minimum mass of 1.9 $M_\oplus$. They also presented a dynamical stability analysis of the system. In particular, the addition of the 3.15d planet, GJ 581e, greatly strengthened the inclination limit for the system. The planet was quickly ejected for system inclinations less than 40°. This dynamical stability constraint implies an upper limit of 1.6 to the $1/\sin i$ correction factor for any planet's minimum mass (assuming coplanar orbits). Most recently, Dawson and Fabrycky (2010) published a detailed study of the effects of aliasing on the GJ 581 data set of Mayor09. They concluded that the 67-day period of GJ 581c remains ambiguous, and favored a period of 1.0125 days that produced aliases at both 67 days and 83 days.

The Gliese 581 system exerts an outsize fascination when compared to many of the other exoplanetary systems that have been discovered to date. The interest stems from the fact that two of its planets lie tantalizingly close to the expected threshold for stable, habitable environments, one near the cool edge, and one near the hot edge. We have had GJ 581 under survey at Keck Observatory for over a decade now. In this paper, we bring 11 years of HIRES precision RV data to bear on this nearby exoplanet system. Our new data set of 122 velocities, when combined with the previously published 119 HARPS velocities, effectively doubles the amount of RVs available for this star, and almost triples the time base of those velocities from 4.3 years to 11 years. We analyze the combined precision RV data set and discuss the remarkable planetary system that they reveal.

2. Radial Velocity Observations

The RVs presented herein were obtained with the HIRES spectrometer (Vogt et al. 1994) of the Keck I telescope. Typical exposure times on GJ 581 were 600 seconds,

yielding a typical S/N ratio per pixel of 140. Doppler shifts are measured by placing an Iodine absorption cell just ahead of the spectrometer slit in the converging f/15 beam from the telescope. This gaseous absorption cell superimposes a rich forest of Iodine lines on the stellar spectrum, providing a wavelength calibration and proxy for the point spread function (PSF) of the spectrometer. The Iodine cell is sealed and temperature-controlled to 50 ± 0.1 C such that the column density of Iodine remains constant (Butler et al. 1996). For the Keck planet search program, we operate the HIRES spectrometer at a spectral resolving power R $\approx$ 70,000 and wavelength range of 3700 – 8000 Å, though only the region 5000 – 6200 Å (with Iodine lines) is used in the present Doppler analysis. Doppler shifts from the spectra are determined with the spectral synthesis technique described by Butler et al. (1996). The Iodine region is divided into $\sim$700 chunks of 2 Å each. Each chunk produces an independent measure of the wavelength, PSF, and Doppler shift. The final measured velocity is the weighted mean of the velocities of the individual chunks.

In August 2004, we upgraded the focal plane of HIRES to a 3-chip CCD mosaic of flatter and more modern MIT-Lincoln Labs CCD's. No zero point shift in our RV pipeline was incurred from the detector upgrade. Rather, the new CCD mosaic eliminated a host of photometric problems with the previous Tek2048 CCD (non-flat focal plane, non-linearity of CTE, charge diffusion in the silicon substrate, overly-large pixels, and others). The deleterious effects of all these shortcomings can be readily seen as larger uncertainties on the pre-August 2004 velocities.

In early 2009, we submitted a paper containing our RVs up to that date for GJ 581 that disputed the 83-day planet claim of Mayor09. One of the referees (from the HARPS team) kindly raised the concern (based partly on our larger value for apparent stellar jitter) that we may have some residual systematics that could be affecting the reliability of some of our conclusions. In the precision RV field there are no suitable standards by which

teams can evaluate their performance and noise levels; so, it is rare but also extremely useful for teams to be able to check each other using overlapping target stars, like GJ 581, for inter-comparison. So, we took the HARPS team's concerns to heart and withdrew our paper to gather another season of data, to do a detailed reanalysis of our uncertainty estimates, and to scrutinize our 15-year 1500-star data base for evidence of undiscovered systematic errors.

Soon after we withdrew our 2009 paper, Mayor09 published a revised model wherein they altered their 83-day planet period to 66.8 days (citing confusion by yearly aliases) and also announced an additional planet in the system near 3.15 days. For our part, as a result of our previous year's introspection, we discovered that the process by which we derive our stellar template spectra was introducing a small component of additional uncertainty that added about 17% to our mean internal uncertainties. This additional noise source stems from the deconvolution process involved in deriving stellar template spectra. This process works quite well for G and K stars, but it is prone to extra noise when applied to heavily line-blanketed M dwarf spectra. We have included this in our present reported uncertainties for GJ 581, and are working on improvements to the template deconvolution process. Furthermore, our existing template for this star, taken many years ago, was not up to the task of modeling RV variation amplitudes down in the few ms^{-1} regime. So, over the past year, we obtained a much higher quality template for GJ 581.

The HIRES velocities of GJ 581 are presented in Table 1, corrected to the solar system barycenter. Table 1 lists the JD of observation center, the RV, and the internal uncertainty. The reported uncertainties reflect only one term in the overall error budget, and result from a host of systematic errors from characterizing and determining the PSF, detector imperfections, optical aberrations, effects of under-sampling the Iodine lines, etc. Two additional major sources of error are photon statistics and stellar jitter. The former is

already included in our Table 1 uncertainties. The latter varies widely from star to star, and can be mitigated to some degree by selecting magnetically-inactive older stars and by time-averaging over the star's unresolved low-degree surface p-modes. The best measure of overall precision for any given star is simply to monitor an ensemble of planet-free stars of similar spectral type, chromospheric activity, and apparent magnitude, observed at similar cadence and over a similar time base. Figures 2, 3, and 4 of Butler et al. (2008) show 12 M dwarfs with B-V, V magnitude, and chromospheric activity similar to GJ 581. In any such ensemble, it is difficult to know how much of the root-mean-square (RMS) of the RVs is due to as-yet-undiscovered planets and to stellar jitter. However, these stars do establish that our decade-long precision is better than 3 ms^{-1} for M dwarfs brighter than V=11, including contributions from stellar jitter, photon statistics, undiscovered planets, and systematic errors.

3. Properties of GJ 581

The basic properties of GJ 581 were presented by Bonfils05 and Udry07 and will, for the most part, simply be adopted here. Briefly recapping from Bonfils05 and Udry07, GJ 581 is an M3V dwarf with a parallax of 159.52 ± 2.27 mas (distance of 6.27 pc) with V = 10.55 ± 0.01 and B-V = 1.60. The parallax and photometry yield absolute magnitudes of M_V = 11.56 ± 0.03 and M_K = 6.86 ± 0.04. The V-band bolometric correction of 2.08 (Delfosse et al. 1998) yields a luminosity of 0.013 $L_\odot$. The K-band mass-luminosity relation of Delfosse et al. (2000) indicates a mass of 0.31 ± 0.02 $M_\odot$, and the mass-radius relations of Chabrier & Baraffe (2000) yield a radius of 0.29 $R_\odot$. Bean et al. (2006) report the [Fe/H] of GJ 581 to be -0.33, while Bonfils05 report [Fe/H] = -0.25. Both results are consistent with the star being slightly metal-poor, in marked contrast to most planet-bearing stars that are of super-solar metallicity. Johnson & Apps (2009) presented a broadband (V-K)

photometric metallicity calibration for M dwarfs that, in conjunction with the star's broadband magnitudes implies a metallicity of [Fe/H] = -0.049. Most recently, Rojas-Ayala et al. (2010) estimated the metallicity at -0.02, while Schlaufman and Laughlin (2010) cite a metallicity of -0.22. Thus, GJ 581 appears to be basically of solar or slightly sub-solar metallicity, yet has produced at least 4 or more low-mass planets. However, this is no cause for surprise. Laughlin et al. (2004) and Ida & Lin (2005) have argued that the formation of low-mass planets should not be unduly affected by modestly subsolar metallicity.

Udry07 report GJ 581 to be one of the least active stars on the HARPS M-dwarf survey, with Bonfils05 reporting line bisector shapes stable down to their measurement precision levels. Udry07 report a measured $v \sin i \leq 1$ kms^{-1}. They thus find GJ 581 to be quite inactive with an age of at least 2 Gyr. Our measurement of $\log R'_{hk} = -5.39$ leads to an estimate (Wright 2005) of 1.9 ms^{-1} for the expected RV jitter due to stellar surface activity and an age estimate of 4.3 Gyr.

4. Photometric Observations

Precise photometric observations of planetary host candidate stars are useful to look for short-term, low-amplitude brightness variability due to rotational modulation in the visibility of starspots and plages (see, e.g., Henry, Fekel, & Hall 1995). Long-term brightness monitoring of these stars enabled by our automatic telescopes can detect brightness changes due to the growth and decay of individual active regions as well as brightness variations associated with stellar magnetic cycles (Henry 1999; Lockwood et al. 2007; Hall et al. 2009). Therefore, photometric observations of planetary candidate stars help to determine whether the observed radial velocity variations are caused by stellar activity (spots and plages) or reflex motion due to the presence of orbiting companions. Queloz et al. (2001) and Paulson et al. (2004) have documented several examples of solar-type stars whose periodic radial

velocity variations were caused by stellar activity.

GJ 581 has also been classified as the variable star HO Librae, though Weis (1994) reported its short-term variability to be at most 0.006 magnitudes. Udry07 report the star to be constant to within the 5 millimag Geneva photometry catalog precision of V=10.5 stars.

We acquired new photometric observations of GJ 581 in the Johnson V band during the 2007 and 2008 observing seasons with an automated 0.36 m Schmidt-Cassegrain telescope coupled to an SBIG ST-1001E CCD camera. This Tennessee State University telescope was mounted on the roof of Vanderbilt University's Dyer Observatory in Nashville, Tennessee.

Differential magnitudes were computed from each CCD image as the difference in brightness between GJ 581 and the mean of four constant comparison stars in the same field. A mean differential magnitude was computed from usually ten consecutive CCD frames. Outliers from each group of ten images were removed based on a 3σ test. If three or more outliers were filtered from any group of ten frames (usually the result of non-photometric conditions), the entire group was discarded. One or two mean differential magnitudes were acquired each clear night; our final data set consists of 203 mean differential magnitudes spanning 530 nights.

Our 203 photometric observations are plotted in the top panel of Figure 1; they scatter about their mean with a standard deviation of 0.0049 mag. A periodogram of the observations, based on least-squares sine fits, is shown in the second panel, resulting in a best-fit period of 94.2 $\pm$ 1.0 days. That rotation period is quite similar to the rotational period of another important M dwarf planet host, GJ 876, and gives added confidence to the current findings. It is also consistent with GJ 581's low activity and age estimate. In the third panel, we plot the observations modulo the 94.2-day photometric period, which we take to be the star's rotation period. A least-squares sine fit on the rotation period gives

a semi-amplitude of 0.0030 ± 0.0004 mag. The window function for the rotation period is plotted in the bottom panel. Five of the six radial velocity periods discussed below are indicted by vertical dotted lines in the second and fourth panels; our data set is not long enough to address the 433-day period of GJ 581f. As will be shown below, none of the five periods coincide with any significant dip in the periodogram.

5. Orbital Analysis

We obtained 122 RVs with the HIRES spectrometer at Keck. The data set spans 10.95 years with a peak-to-peak amplitude of 37.62 ms^{-1}, an RMS velocity scatter of 9.41 ms^{-1}, and a mean internal uncertainty of 1.70 ms^{-1}. Figure 2 (top panel) presents the RVs tabulated in Table 1, combined with the HARPS RVs published by Mayor09. The 122 (red) hexagon points are the HIRES observations, while the HARPS observations are shown as (blue) triangle points. A zero-point offset of 1.31 ms^{-1} was removed between the two data sets, and Figure 2 has this offset included. The HARPS data consist of 119 observations at a reported median uncertainty of 1.10 ms^{-1} and extending over 4.3 years. The peak-to-peak amplitude of the HARPS data set is 39.96 ms^{-1}. The combined data set has 241 velocities, with a median uncertainty of 1.30 ms^{-1}.

For the orbital fits, we used the SYSTEMIC Console (Meschiari et al. 2009; Meschiari & Laughlin 2010). We assume coplanar orbits with $i = 90°$ and $\Omega = 0°$. Uncertainties are based on 1000 bootstrap trials. We take the standard deviations of the fitted parameters to the bootstrapped RVs as the uncertainties in the fitted parameters. The fitted mean anomalies are reported at epoch JD 2451409.762. The assumed mass of the central star is $0.31 M_{\odot}$. For all fits presented here, we fixed the eccentricities at zero since the amplitudes are all quite small and extensive modeling revealed that allowing eccentricities to float for any or all of the 6 planets does not significantly improve the overall fit.

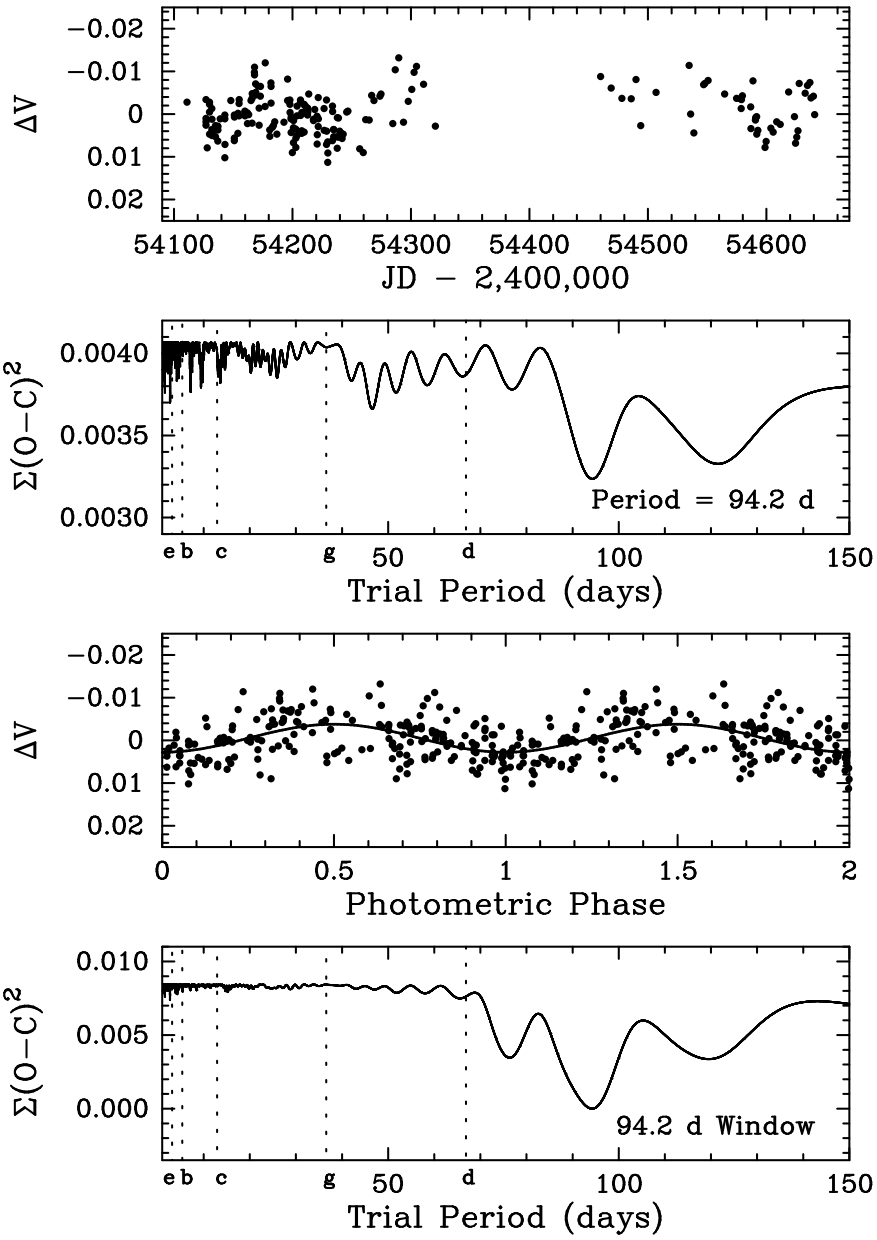

Fig. 1.— (*Top*): Photometric V-band observations of GJ 581 acquired during the 2007 and 2008 observing seasons with an automated 0.36 m imaging telescope. (*Second Panel*): Periodogram analysis of the observations gives the star's rotation period of 94.2 days. (*Third Panel*): The photometric observations phased with the 94.2-day period reveal the effect of rotational modulation in the visibility of photospheric starspots on the brightness of GJ 581. (*Bottom*): Window function of the 94.2-day rotation period. The radial velocity periods of 5 of the 6 planetary companions are indicated by vertical dotted lines in the second and fourth panels.

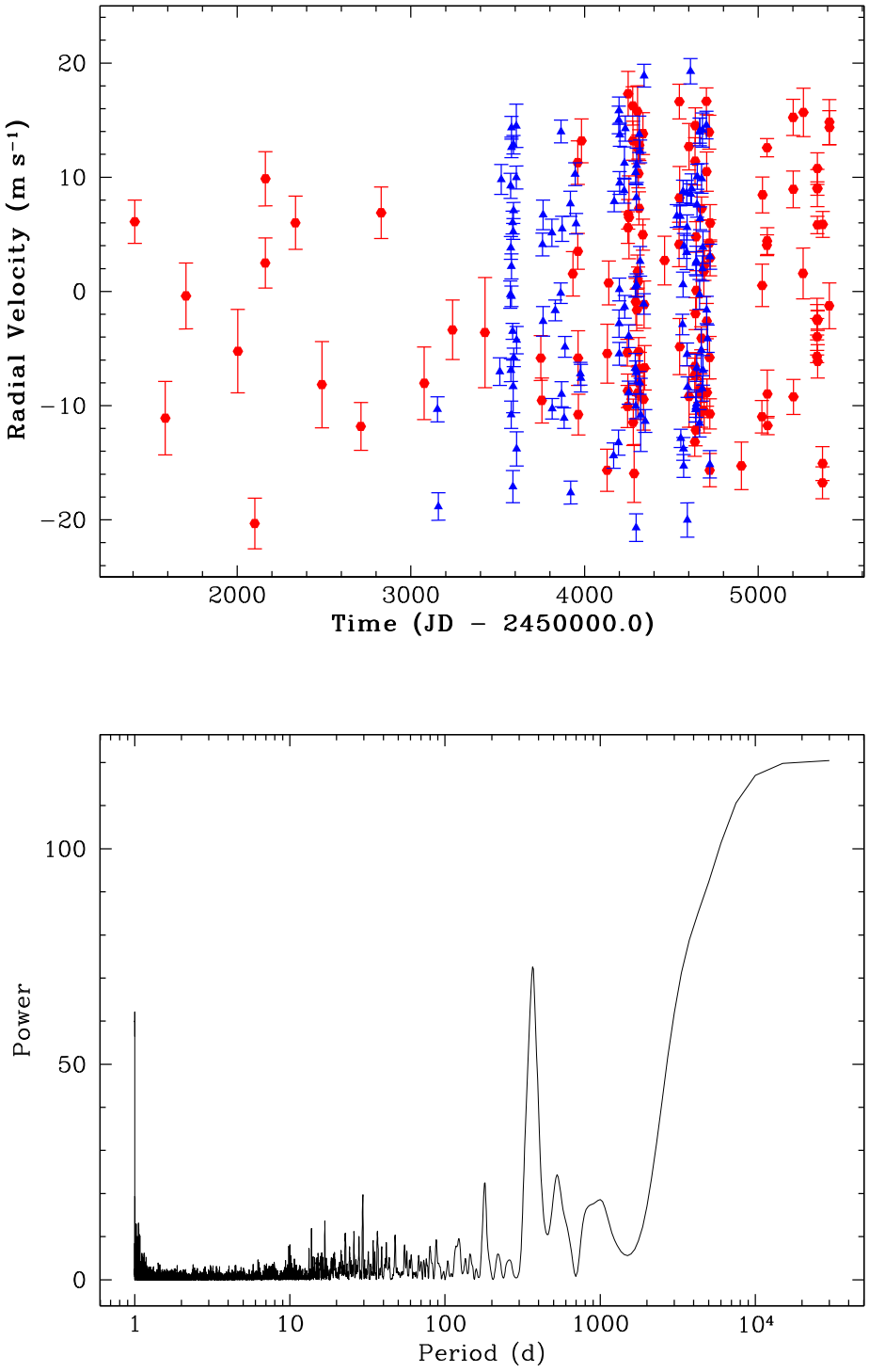

Fig. 2.— Top panel: Combined RV data of GJ 581 from HIRES (red hexagons) and HARPS (blue triangles). Lower panel: spectral window

The power spectrum of the sampling window is shown in the lower panel of Figure 2. As expected, there is some spurious power created by the sampling times near periods of 1.003d (the solar day in sidereal day units), 29.5d (the lunar synodic month), 180d (∼1/2 year), and 364d (∼1 year), all artifacts of the nightly, monthly, and yearly periods on telescope scheduling.

The top panel of Figure 3 shows the power spectrum of the RV data. Following Gilliland & Baliunas (1987) (hereafter GB87), in Figure 3, we use an error-weighted version of the Lomb-Scargle periodogram. The horizontal lines in the periodograms in Figure 3 roughly indicate the 0.1%, 1.0%, and 10.0% False Alarm Probability (FAP) levels from top to bottom. To determine better estimates of the FAPs of the prominent peaks in the periodograms, we define the noise-weighted power in a prominent peak with (GB87)

$$p_0 = \frac{N}{4}\frac{x_0^2}{\sigma_0^2}, \tag{1}$$

where N is the number of observations, x_0 is the RV half-amplitude implied by the peak, and σ_0^2 is the variance in the data or residuals prior to fitting out the implied planet. Additionally, we can also define power in a prominent peak as (Cumming (2004)):

$$p_0 = \frac{(N-2)}{2}\frac{(\chi^2_{\rm constant} - \chi^2_{\rm circ})}{\chi^2_{\rm circ}}, \tag{2}$$

where $\chi^2_{\rm circ}$ is the reduced chi-squared for a circular fit at/near the period implied by the peak and $\chi^2_{\rm constant}$ is the reduced chi-squared for a constant RV model of the data or residuals.

Estimation of the false-alarm probability of a given peak requires knowledge of the number of independent frequencies, M in the data set. Given the highly uneven sampling, M considerably exceeds our $N = 241$ Doppler velocity measurements. Using the Monte-Carlo procedure outlined by Press et al. (1992), we find that $M = 2525$.

The FAP is the chance that a peak as high as, or higher than, that observed in the

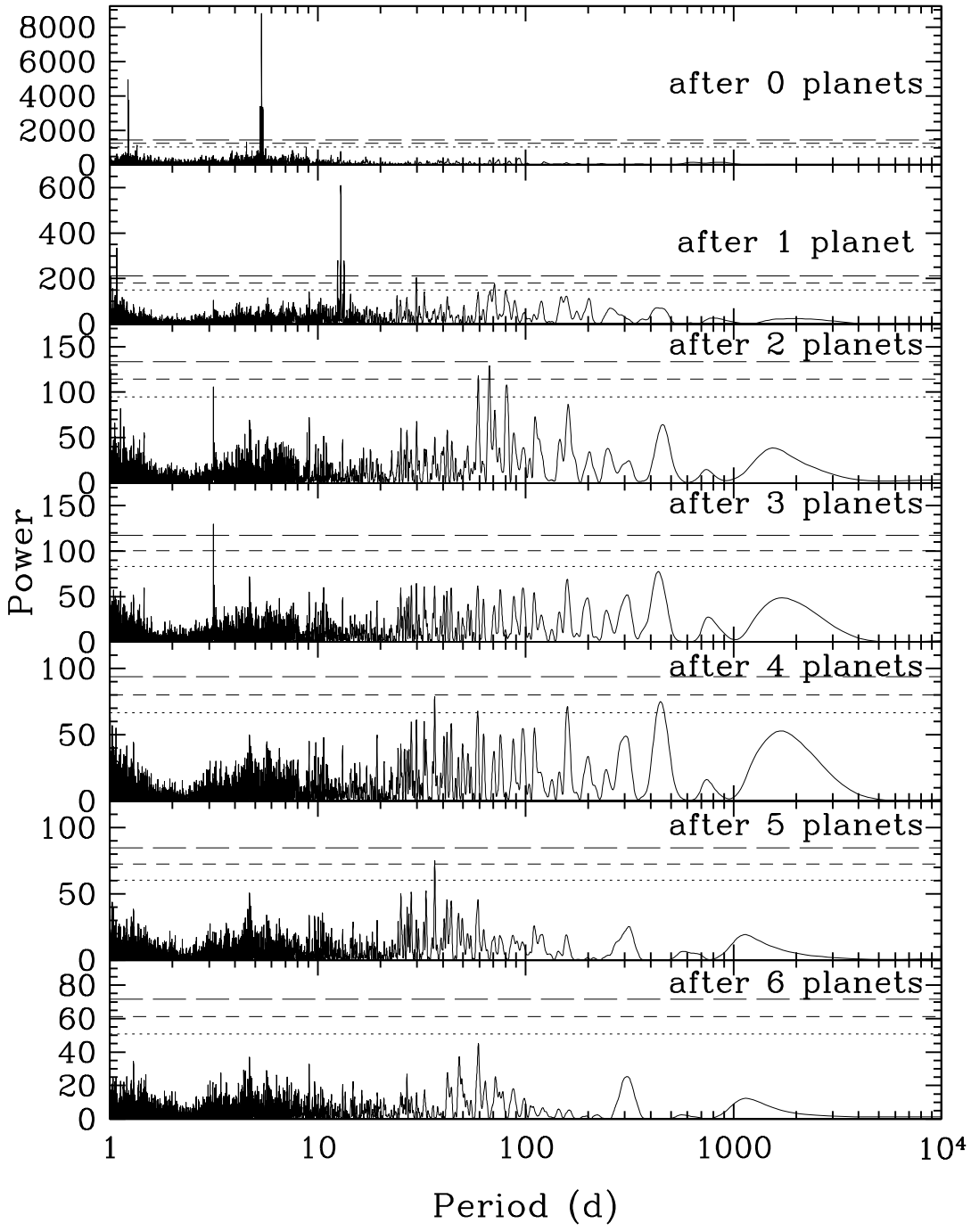

Fig. 3.— From top to bottom, power spectra of the residuals to the 0-, 1-, 2-, 3-, 4-, 5-, and 6-planet solutions, respectively. The horizontal lines in each periodogram roughly indicate the 0.1%, 1.0%, and 10.0% False Alarm Probability (FAP) levels from top to bottom.

periodogram would occur by chance,

$$Pr(p_0, M) = 1 - [1 - \exp(-p_0)]^M \,. \tag{3}$$

In general, we find that M is roughly the same for both definitions of p_0 above.

Note that there are discrepancies between our FAPs quoted below and the FAP lines shown in Figure 3. Here we explain the reasons for these discrepancies. The (raw) power levels shown in Figure 3 are based on Equations 1 and 2 in GB87. The FAP lines are based on the method to calculate the number of degrees of freedom, M, suggested in Section 13.7 of Press et al. (1992), except that we assume a Gaussian distribution with a standard deviation equal to the velocity scatter of the data or residuals. However, the FAPs we quote below for each fitted planet are for power levels defined by Equation 2 above.

Figure 3 shows the power spectra of the residuals of the RV data from the best Keplerian fits for models with n planets (with n ranging from 0 to 6). The eccentricities are held fixed at 0 throughout the fitting process. The dominant spike in the top panel is at 5.368 days and is the well-known Hot-Neptune (GJ 581b) first reported by Bonfils05. The power implies a minimum-mass $m \sin i$ =15.6 $M_\oplus$ companion in a 0.041 AU orbit. The reduced chi-squared statistic (using 5 free parameters) for this 1-planet fit is 8.426, with an RMS of 3.65 ms^{-1}. The estimated FAP is 6.8×10^{-306}, in keeping with the extremely strong detection.

The second panel down in Figure 3 shows the power spectrum of the residuals to the 1-planet fit. This power spectrum is dominated by a peak at 12.92 days. A 2-planet fit for the 12.92-day peak (planet-c first reported by Udry07) reveals a minimum-mass 5.5 $M_\oplus$ planet in a 0.073 AU orbit. The 2-planet fit achieves a reduced chi-squared statistic (using 8 free parameters) of 4.931, and an RMS of 2.90 ms^{-1}. The estimated FAP is 2.3×10^{-33}. So, the 12.92-day planet-c first reported by Udry07 also seems well-confirmed.

The third panel down of Figure 3 shows the power spectrum of the residuals of the 2-planet model. As Mayor09 found, the next obvious peak to fit is the maximum peak in the group near 67 days. Mayor09 found that this group is a set of 3, with the true peak at 67 days, and 1-year aliases near 59 and 82 days ($1/67 - 1/365 \sim 1/82$, and $1/67 + 1/365 \sim 1/57$). We explored various fitting branches involving the 59d and 82d peaks for planet d. Fitting for the 59-day peak left pronounced residuals at both 67 and 82 days. Fitting out the 82-day peak left pronounced residual peaks near 59 days, 37 days and 158 days. Neither the 59-day nor the 82-day fitting branches led to final solutions that were as good as the 67-day branch. We therefore concur with Mayor09 that the 67-day is the correct choice for planet d. A fit to the 66.9-day peak indicates a minimum-mass $4.4\,M_{\oplus}$ planet in a 0.218 AU orbit. The 3-planet fit results in a reduced chi-squared statistic (using 11 free parameters) of 4.207, with an RMS of 2.72 ms^{-1}. The estimated FAP is 2.5×10^{-6}. Thus, the 67-day 3rd planet announced by Mayor09 seems well-supported by the present data set.

At this point, there are also similar-power peaks present very near 1.00 day, both above and below. These "near-1-day" peaks appear frequently in our RV data sets and typically arise from aliasing effects, as discussed in detail by Dawson and Fabrycky (2010). They are due partly to the fact that exoplanet observations are done only at night. Dawson and Fabrycky (2010) looked carefully at the HARPS data set for GJ 581 and concluded that it remains unclear whether the period of GJ 581d is 67 days, or 83 days, or even their preferred value of 1.0125 days, and that further observations were required to resolve the ambiguity. In our experience, RV power from a star being orbited by legitimate planets roughly in the 20 – 90 period range can feed substantial amounts of that power into peaks very near 1.00 day, by beating with the sidereal and solar days. Thus, while it may be possible on rare occasion to encounter a true planet orbiting a given star with a period very near 1.00 day, this will be the exceptional case, and not very compelling from a purely

Bayesian point of view. In addition, one can only use this alternative once in a system to explain away a suspected planet peak up at a longer period. Multiple longer period peaks would require multiple planets at or very near 1.00 day, and that is dynamically untenable.

To look into this more carefully, we intentionally obtained some extended cadence over the course of nights on May 21-25, June 21-23, and again on July 30-31, 2010. We then carefully examined the periodogram of the residuals of the two-planet fit. The periodogram has two prominent peaks at 66.9645 days and 1.0126 days with raw powers of 129.070 and 124.310, respectively. The ratio of the power levels is 1.038. We generated mock RV sets based on two models. First, we took the three-planet fit with the third planet at 1.0126 days and scrambled the residuals 1000 times. We fit two planets to each mock RV set. We then examined the periodograms of the residuals. In particular, we measured how frequently the ratio of the power levels at the two periods exceeds 1.038. Then we repeated this procedure with the third planet at 67 days. We found that the 67-day model does an overwhelmingly better job at producing periodograms which resemble the periodogram of the actual residuals. Our Monte Carlo results indicate a 93.6% probability that 67 days is the correct period.

The fourth panel of Figure 3 shows the periodogram of the residuals from the 3-planet fit. As was found also by Mayor09, the next obvious peak to fit is the 3.15-day one, previously reported by Mayor09. A Keplerian fit to this peak indicates a planet in a 0.028 AU orbit with a period of 3.149 days and minimum mass of only $1.7\,M_{\oplus}$ (smaller by about 10% than that found by Mayor09). The 4-planet fit achieves a reduced chi-squared statistic (using 14 free parameters) of 3.463 and an RMS of 2.43 ms^{-1}. The estimated FAP of the peak is 1.9×10^{-8}. So, the 3.15-d planet-e announced by Mayor09 also seems well-confirmed by the combined data set and may even be about 10% lower in mass than first reported.

The fifth panel down in Figure 3 shows the periodogram of the residuals to our best

4-planet fit. Here, there are two (nearly) equal power peaks in the residuals power spectrum, near 37 days and 445 days. In general, our experience has shown that it is much harder, with a given data set, to generate coherent power at longer periods. So, between two peaks of equal power, the one with the longer period is usually more significant. So, we fit the 445-day peak next, though the remaining branches of the fitting tree and final solution are not significantly altered by fitting the 37-day peak first instead. A fit to the 445-day peak indicates a minimum-mass $6.8\,M_{\oplus}$ planet in a 443-day 0.770 AU orbit. The 5-planet fit achieves a reduced chi-squared statistic (using 17 free parameters) of 2.991 and an RMS of 2.30 ms^{-1}. The estimated FAP of the peak is 9.5×10^{-5}. This 5th planet thus appears statistically well-justified by the present data set.

The sixth panel down in Figure 3 shows the periodogram of the residuals to the 5-planet fit. A lone dominant peak remains near 37 days. This peak shows the extreme narrowness expected of a truly coherent signal, that, if Keplerian and real, would have a strictly fixed period and phase for its 110 cycles spanning the past 11 years of the data set. A fit to this peak indicates a planet of minimum-mass $3.1\,M_{\oplus}$, on a 36.56-day orbit of size 0.146 AU. Our best 6-planet fit (again, assuming circular orbits) achieves a reduced chi-squared statistic (using 20 free parameters) of 2.506 and an RMS of 2.12 ms^{-1}. The estimated FAP of the $\sim$37-day peak is 2.7×10^{-6}. Thus, this 6th planet also seems statistically well-justified by the present data set.

Finally, the bottom panel of Figure 3 shows the periodogram of the residuals of the 6-planet fit. This 6-planet model leaves no remaining peaks of consequence to fit at this time. The residual peak near 59 days has been visible all the way up the stack of panels in Figure 3 and is apparently associated with the yearly alias involved with the 67-day, as pointed out by Mayor09. It has a FAP (using the definition for power in Equation 1) of only 0.186. The phased curve at this period shows significant phase gaps in both the

HARPS and HIRES data sets due to the constraint of spectroscopic observations of bright stars mostly receiving only bright or grey lunar time. Such phase gaps further increase the chances of a false alarm here. A 59-day planet is also completely dynamically untenable (even with the assumption that all orbits are circular).

We wondered how many of these planets are independently confirmed by each data set. This is difficult to answer as the Keplerian fitting tree process does not hold previous planets fixed as the next planet is optimized in the process. So we looked at running the fitting process backwards. For each independent HARPS and HIRES data set, we subtracted our model of the system (as listed in Table 2) from the data, giving a set of residuals. The reflex motions corresponding to the planets in our RV model were then added back in sequentially. The advantage to this approach is that there is no optimization and resulting parameter drift between periodograms, and one sees the sometimes non-intuitive result of adding a known signal. This process showed us that the characterization of the system requires the combination of both data sets.

Figure 4 shows this reverse sequence of injecting best-fit stellar reflex motion at each Keplerian period back into velocity residuals for each data set. The set of panels on the left show the sequence for the HIRES data set, while the panels on the right show the same sequence for the HARPS data set. The top panel on each side shows the periodogram of the residuals after fitting out all 6 planets. In each successive panel, the period of the injected signal is denoted by a red vertical tick mark.

The second panel on the left of Figure 4 shows the effect of injecting the 37-day signal into the HIRES residuals. The 37-day signal is clearly visible in the HIRES data set alone and manifests at the correct period. The 3rd panel on the left of Figure 4 reveals that the 433-day signal is also visible and also manifests near its true period. The 4th panel on the left illustrates that adding in the 3.15-day signal generates power primarily at the

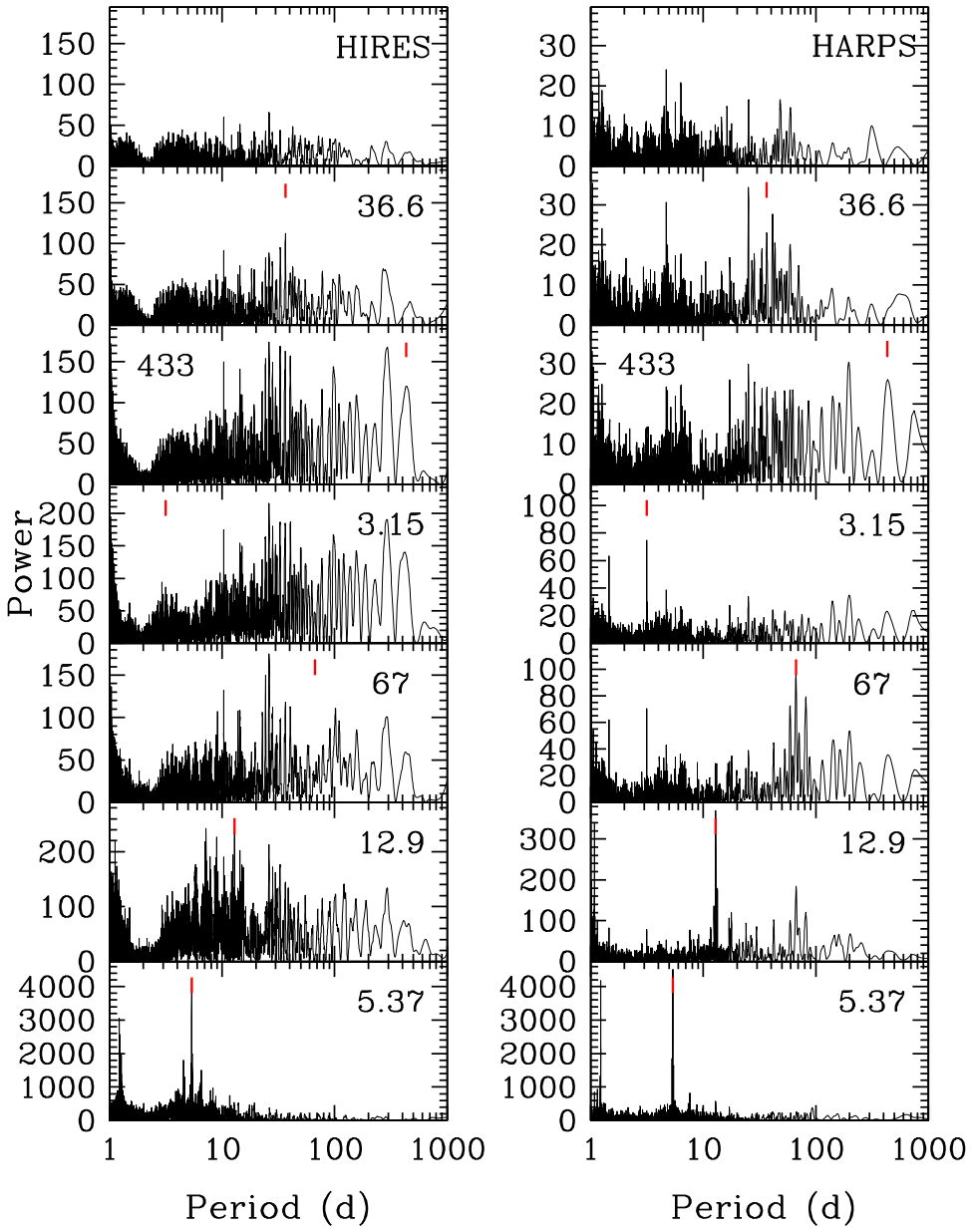

Fig. 4.— The effect of sequentially adding signal in reverse order at each Keplerian period back into the residuals of each data set for GJ 581. Panels on the left show the results for the HIRES data set, while those on the right show the results for the HARPS data set. The top panels show the periodograms of the residuals from the 6-planet fit. The annotations and red vertical tick marks in each panel indicate the period of the last injected signal prior to computing each periodogram.

non-intuitive period of about 26 days. The spectral window of the HIRES sampling times has peaks at 29.53, 363.24, 1.003, and 179.72 days. This 26-day peak could thus be drawing power from at least three sources 1) a lunar alias of the 36.6-day planet, 2) a half-year alias of the 66.9-day planet, and 3) both a one-day and a half-year alias of the 3.15-day planet. These aliasing and sampling effects produced by the particular HIRES data time stamps render the 3.15-day planet inconspicuous in the power spectrum of the HIRES data taken alone. The 5th panel on the left reveals that injecting the 67-day signal makes the situation more confusing, by introducing more peaks. This demonstrates that the combination of both data sets is required to see this planet clearly, apparently because it is near an integer multiple of the lunar month which results in difficulties getting complete phase coverage. The 6th panel on the left shows that injecting the signal from the 12.9-day planet leads to another curious result, producing power at several other frequencies aside from the true 12.9-day periodicity. Finally, the bottom panel on the left shows the injection of the 5.4-day planet's signal. Here, the planet's amplitude is so large that its signal is overwhelmingly manifested at the proper period.

For the HARPS data set alone, the 2nd panel on the right in Figure 4 shows that injecting the 37-d signal generates power instead near 23 days when viewed through the complex filter of time stamps and uncertainties specific to the HARPS data points. Apparently, the HARPS data set alone is not able to reliably sense this planet. The 3rd panel on the right illustrates that adding in the 433-day signal generates power both near 433 and at its yearly alias near 200 days. The 4th panel on the right shows that the injected signal from the 3.15-day planet also manifests well in the HARPS data set alone and does not generate power at 26 days as happened with the HIRES data set. This is apparently a result of many of their observing runs that garnered long blocks of contiguous nights with high and sustained cadence. The 5th panel on the right shows that the signal injected from the 67-day period shows up very well and at the expected period, flanked also by its yearly

aliases near 59 and 82 days. The 6th and 7th panels on the right show that the signals from the 12.9-day and 5.4-day planets also manifest quite reliably in the HARPS data set alone.

So, in summary, it is clear that, although most of these planet signals do show up independently in each data set, the situation is confused by aliasing with peaks in the spectral window caused by the specific time stamps unique to each data set. It is really necessary to combine both data sets to sense all these planets reliably.

A summary of our best Keplerian fit with (forced) circular orbits is presented in Table 2. The fitted mean anomalies are reported at epoch JD 2451409.762. The final parameters shown here are slightly different than those quoted for the fits along the fitting tree and represent our best overall model. Uncertainties (in parentheses) on each quantity are determined from 1000 bootstrap trials from which we take the standard deviations of the fitted parameters to the bootstrapped RVs as the uncertainties. We also calculated uncertainties with a Markov-chain Monte Carlo estimator, and both are in good agreement. The 6-planet all-circular fit achieves a reduced chi-squared parameter of 2.6503 and an RMS of 2.118 ms^{-1}. Allowing eccentricity to float for any or all of the 6 planets did not produce any significant improvement in the overall quality of the fit, either in the reduced chi-squared statistic, in RMS, or in required stellar jitter. Given the very small amplitudes of the signals, it is not altogether surprising that almost all of the fitted eccentricities are statistically consistent with zero.

Our best fit indicates that, if one allows a stellar jitter of 1.4 ms^{-1}, the reduced chi-squared statistic drops to 1.0. This jitter estimate agrees quite well with that of Mayor09, who found a value of 1.2 ms^{-1} from their 4-planet fit. Little is known about the lower bounds of jitter for any star. If the true stellar RV jitter is even less than this, there could yet be more planets in the system that further precision RV data might reveal. But we also find it remarkable that this star's jitter has not exceeded 1.4 ms^{-1} over the

11-year extent of the data and that the entire data set can be fit to this level of precision by only 6 circular orbits (20 free parameters). Backing out the stellar jitter in the quadrature sum implies that, with this data set, we are able to track the motion of the 6 planetary companions around GJ 581 to a precision of 1.6 ms^{-1} over 11 years. Figure 5 shows the phased barycentric reflex velocities of the host star due individually to each companion in the system. Except for the 2nd panel, the ordinate scaling has been held constant to simplify inter-comparison of the various planets.

We also explored many solution sets allowing eccentricities to float for some or all of the planets. As mentioned above, none produced any significant improvement in overall fit quality. Moreover, most models quickly became unstable once eccentricities rose much above 0.2 or so. Our very best eccentric fits benefitted primarily from allowing eccentricity on the 67-day and 37-day planets' orbits with these two planets participating in a secular resonance.

We also carefully examined the effects of including dynamics in the fitting process. The SYSTEMIC Console includes a Gragg-Bulirsch-Stoer integrator that can be used to model planet-planet gravitational interactions. We find that dynamical effects have an insignificant effect on improving the fit presented in Table 2, and the 6-planet system appears dynamically stable over at least a 50 Myr timescale. We also explored the possibility of setting limits on the inclination of the system from dynamical stability experiments. Mayor09 had found that the dynamical stability of their 4-planet system, particularly the stability of the 3.15-day planet, imposed a lower bound of about 40° for the inclination of the system (presumed co-planar). Thus, each of GJ 581's planets could not be more massive than about 1.6 times their minimum mass.

We find that, through stability considerations, all-circular orbit solutions only very weakly constrain the inclination of the system. Planetary masses have to be increased by a

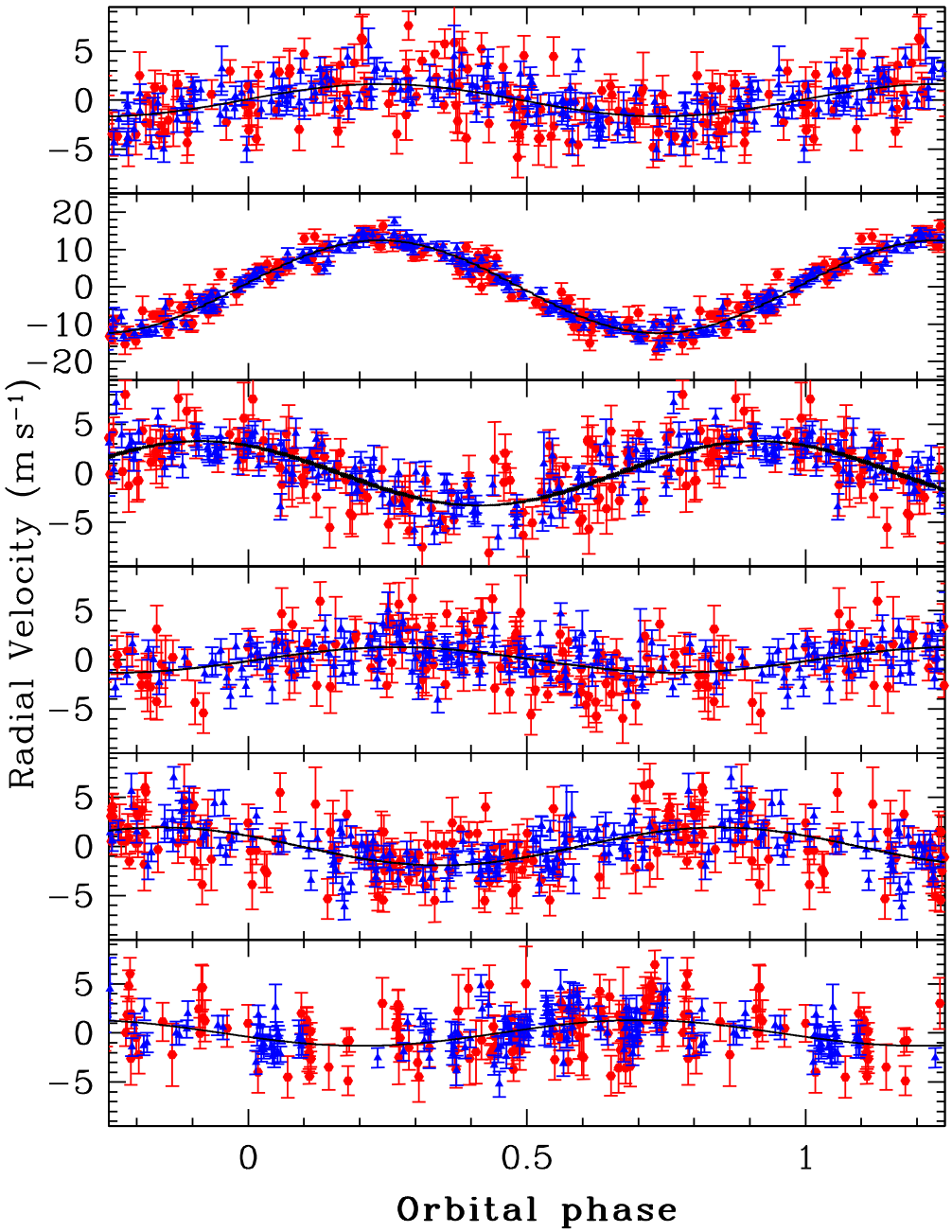

Fig. 5.— Phased reflex barycentric velocities of the host star due individually to the planets at 3.15 days, 5.37 days, 12.9 days, 37 days, 67 days, and 433 days from the all-circular fit of Table 2. Filled (red) hexagon points are from Keck while filled (blue) triangles are from HARPS.

factor > 10 to provoke instability in less than 50 Myr, and that translates to a lower bound on the inclination of only $\sim 6°$. Eccentricities do play a role in setting a lower limit to the inclination. Floating eccentricity solutions with mass factors $(1/m \sin i) > 1.4$ are unstable. Even if only low eccentricities (< 0.2) are allowed in the orbits, an upper limit for $1/m \sin i$ of $1.4-1.5$ is indicated from dynamical stability considerations alone. This implies that, if any of the orbits are eccentric, the system's inclination is likely to be $> 45°$. It seems likely that small eccentricities are probably present in some or even all of these orbits. However, since we cannot prove that small eccentricities are present, the inclination can't yet really be definitively constrained.

Table 3 gives the semi-amplitudes of least-squares sine fits of the photometric observations (Figure 1) corresponding to each of the radial velocity periods modeled in this paper. These upper limits to brightness variability are all very small and supportive of Keplerian motion of planetary companions as the cause of all the radial velocity variations.

Figure 6 shows a simple top view of the system, with the axes labeled in AU. For reference, the orbits of Earth, Venus, and Mercury are overlaid as blue, green, and red dashed lines respectively. The entire GJ 581 system would fit comfortably within the Earth's orbit. And the basic structure of the GJ 581 system (with its nearly all-circular orbits and a tight inner clutch of planets accompanied by a much more distant outer planet) is in some respects eerily reminiscent of the nearly all-circular orbits of our own solar system, with its inner clutch of terrestrial planets and attendant distant Jupiter.

6. Characteristics of the 37-day planet

The GJ 581 system has a somewhat checkered history of habitable planet claims, so a brief historical review of the alleged properties of the various planets in this system

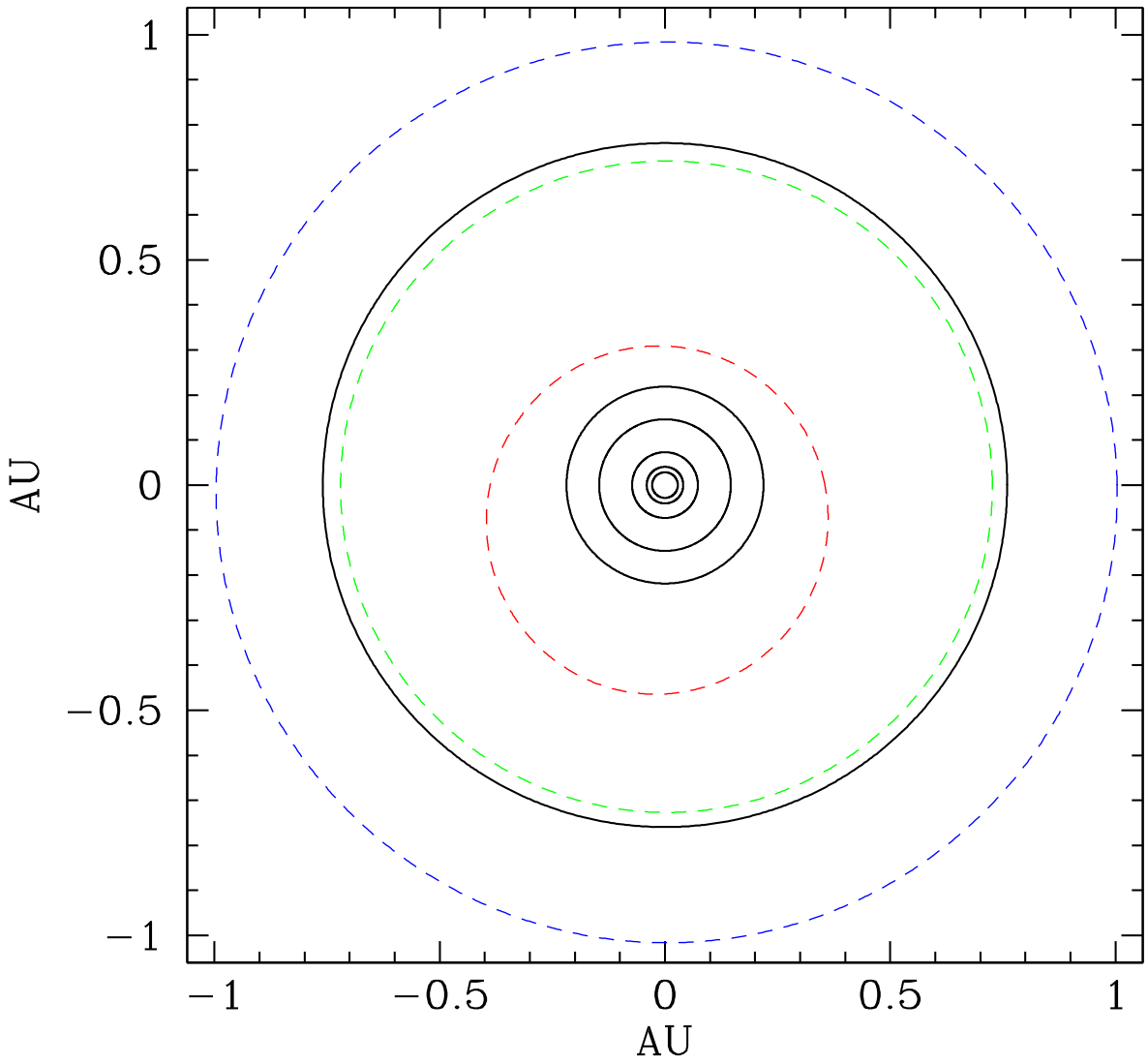

Fig. 6.— Top view of the GJ 581 system. For reference, the orbits of Earth, Venus, and Mercury are overlaid as dashed blue, green, and red lines respectively.

is appropriate. Both the 12.9-day and 83-day planets reported by Udry07 were initially thought likely to be habitable planets. However, further analysis by others (previously described in the introduction) showed that the 12.9-day planet was likely too hot and the 83-day too cold to support habitability. Two years later, when Mayor09 revised the period of the 83-day planet to 67 days, that planet's prospects for habitability increased somewhat, despite the fact that, at a minimum mass of 7.1 $M_{\oplus}$, and a maximum mass of up to 11.4 $M_{\oplus}$, the distinction between a rocky planet and an ice-giant becomes uncertain. The new mass, as derived here is 5.6 – 8.4 $M_{\oplus}$. But even with a Bond albedo of 0, at its distance of 0.218 AU from the star, ignoring the effects of the star's spectral energy distribution, that planet's maximum equilibrium temperature would be only 203 K.

However, if confirmed, the 37-day planet candidate offers a solid case for a potentially habitable planet in this very nearby system. The best Keplerian fit to the data indicates a 3.1 $M_{\oplus}$ planet in a circular 36.6-day orbit of semi-major axis 0.146 AU. The dynamical stability investigations presented by Mayor09 also impose a lower bound on the orbital plane inclination, constraining the upper bound on the mass of GJ 581g to be no more than 1.6 times its minimum mass. We find a similar bound of about 1.4 assuming none of the orbital eccentricities exceed 0.2. So, the likely mass for this planet candidate is 3.1 – 4.3 $M_{\oplus}$. Using the results of Seager et al. (2007), the radius of GJ 581g is expected to be 1.3 – 1.5 $R_{\oplus}$ if homogeneous and composed primarily of the perovskite phase of $MgSiO_3$ (Earth-like), or 1.7 – 2 $R_{\oplus}$ if water-ice. All radii are predicted to be ∼20% smaller if the planet is differentiated, so the planet is likely to have a radius below 1.5 $R_{\oplus}$. The mass and radius estimates imply a surface gravity of $\sim$ 1.1 – 1.7 g, very near that of the Earth.

Selsis et al. (2007) offer a detailed summary of conditions for exoplanet habitability, with specific reference to the GJ 581 system, but cautioned that there are many factors that affect habitability. Distance from the star is but one of these factors. A planet may not have

formed with or retained sufficient water. Gravity may be too weak to hold an atmosphere against photodissociative-escape processes. The planet might maintain an active geological cycle to replenish atmospheric CO_2. Or a planet may have accreted a massive H_2 - He envelope that would keep the surface pressure too high to prevent water from existing near the surface in liquid form. Selsis et al. (2007) argue that avoiding the last two scenarios requires a planet's mass to be roughly in the range of $0.5-10\ M_{\oplus}$. GJ 581g easily satisfies this mass condition.

Selsis et al. (2007) also make the point that a necessary and sufficient condition for habitability is that T_{eq} must be lower than about 270 K. The equilibrium temperature (Selsis et al. 2007) is given by $T_{eq}^4 = L\ (1\text{-}A)\ /(16\ \pi\ a^2\ \sigma)$, where σ is the Stefan-Boltzmann constant, a is the orbital radius, and A is the Bond albedo (the fraction of power at all wavelengths scattered back into space). This formula assumes a spherical planet with the energy that is absorbed over the starlit hemisphere being uniformly reradiated over the entire surface of the planet. The Bond albedo does not however depend solely on the geometric and physical characteristics of the planet, but also on the spectral energy distribution of the host star. M stars emit a large amount of their radiation in the infrared. As a result, since the greenhouse effect works by absorbing infrared radiation, the surface temperatures would be higher than predicted by such simple calculations. The thickness, density, and composition of the atmosphere also significantly influence the greenhouse effect. These in turn are ultimately influenced by the planet's mass and radius (its surface gravity) and internal structure. The chaotic processes that operated during the planet's formation and its subsequent evolution determine the planet's mass, radius, and internal structure. So the problem is complex and clearly over-simplified by this formula.

Nevertheless, we estimate the equilibrium temperature given $L_{\star} = 0.0135\, L_{\odot}$ for the host star. We assume a Bond albedo for the planet of A=0.3, a typical value for objects in

the inner Solar System (Earth's Bond albedo is 0.29). For the 36.6-day planet candidate, its semi-major axis of 0.146 AU leads to an equilibrium temperature of 228 K. If instead the Bond albedo is assumed to be 0.5, the equilibrium temperature becomes 209 K. This planet candidate would thus appear to also satisfy another necessary condition for habitability, that $T_{eq} < 270$ K.

An equally important consideration is the actual surface temperature T_s. The equilibrium temperature of the Earth is 255 K, well-below the freezing point of water, but because of its atmosphere, the greenhouse effect warms the surface to a globally-averaged mean value of $T_s = 288$ K. If, for simplicity, we assume a greenhouse effect for GJ 581g that is as effective as that on Earth, the surface temperatures should be a factor 288/255 times higher than the equilibrium temperature. With this assumption, in the absence of tidal heating sources, the average surface temperatures on GJ 581g would be 236 – 258 K. Alternatively, if we assume that an Earth-like greenhouse effect would simply raise the equilibrium temperature by 33 K, similar to Earth's greenhouse, the surface temperature would still be about the same, 242 – 261 K. Since it is more massive than Earth, any putative atmosphere would likely be both denser and more massive. It would be denser because of the larger surface gravity, which would tend to hold more of the atmosphere closer to the surface. And the atmosphere may be significantly more massive if we simply assume that the planet went through a formation process similar to that of the Earth and that all the bodies that went into forming GJ 581g had the same relative amount of gasses as in the bodies that went into making up the Earth. Some of these gases would subsequently be outgassed to make the atmosphere. Note however, that the amount of outgassing can depend critically on the (evolving) internal structure of the planet. More simply, the rocks that hold the gases in GJ 581g will have experienced different pressures and temperatures than those in the Earth. In turn, this determines how easily the gases would be released.

Gliese 581g is likely to have evolved to a spin-synchronous configuration, leading to one hemisphere of the planet lying in perpetual darkness. Joshi et al. (1997) presented three-dimensional simulations of the atmospheres of synchronously rotating planets in the habitable zones of M dwarfs and concluded that such tidally-locked planets can support atmospheres over a wide range of conditions, and despite constraints involving stellar activity, are very likely to remain viable candidates for habitability. Joshi (2003) presented a more sophisticated three-dimensional global atmospheric circulation model that expanded on the previous work of Joshi et al. (1997) and evaluated the climate of a spin-synchronous planet orbiting an M dwarf star. The results of that study reinforced the conclusions of Joshi et al. (1997) that synchronously rotating planets within the circumstellar habitable zones of M dwarf stars should be habitable.

7. Implications for $\eta_\oplus$

In recent years, the parameter $\eta_\oplus$ has been minted by the NASA community to aid in evaluating and planning for space missions that seek to discover habitable planets. The official definition of $\eta_\oplus$ is given by the Exoplanet Task Force Report (Lunine et al. 2008) as: "The fraction of stars that have at least one potentially habitable planet. The Task Force defines a potentially habitable planet as one that is close to the size of the Earth and that orbits within the stellar habitable zone. Close to Earth-sized means between 1/2 and twice the radius of the Earth or in terms of mass between $0.1-10$ times the mass of the Earth. These two definitions are equivalent if a fixed density equal to that of the Earth is adopted."

If confirmed, the discovery of GJ 581g, a planet of $1.3-2\,R_\oplus$ orbiting in the habitable zone of such a nearby star implies an interesting lower limit on $\eta_\oplus$ as there are only ~ 116 known solar-type or later stars (Turnbull & Tarter 2003) out to the 6.3 parsec distance of GJ 581. The definition of $\eta_\oplus$ does not exclude our own Solar system from consideration,

so among that volume-limited sample out to 6.3 pc, we would now know of two habitable systems, GJ 581 and our own solar system, implying $\eta_\oplus$ is at least 2/116 or 1.7%. But not all of these nearest 116 stars have been under survey long enough and with enough cadence to discern such rocky planets. The first planet found around GJ 581, a 16.6 $M_\oplus$ ice-giant, required 20 observations to detect (Bonfils05). The next two planets, a 12.9-day $5M_\oplus$ planet, and an 83-day $8M_\oplus$ planet, required 50 observations over a time span of 1050 days (Udry07). Even so, the orbital periods and minimum masses of both planets required significant revision when additional observations by Mayor09 brought the total to 119 over a time span of 1570 days. The two new planets presented here required over 240 observations to discern. So it would seem that at least ∼200 observations are required to reliably detect and characterize a few-earth-mass planet in the habitable zone of a nearby K or M dwarf.

To the best of our knowledge, only ∼61 of these 116 nearest stars have published evidence of being monitored by our LCES programs and/or by various similar programs involving CPS, HARPS, CORALIE, HET, UVES, CFHT, etc., and only 9 of these are known to us as having enough observations (> 200) to have a reasonable chance at being able to detect such small amplitude signals. So, the current extent of the various RV-based exoplanet surveys implies an incompleteness factor of 116/9 or a factor of 13 increase in the 1.7% lower limit, making $\eta_\oplus$ at least 22%. Looking a little further out, to 10 pc, there are about 302 F, G, K, and M dwarfs. Of these, we could find evidence in the literature for only ∼125 that are under survey and only about 10 of these targeted stars that have more than 200 observations. So, having the Sun and Gliese 581 be the only known habitable exoplanet systems in a volume-limited sample out to 10 pc would imply a lower limit for $\eta_\oplus$ of 2/302 times a survey incompleteness factor or 302/10, or about 20%. Looking further out still, to 12 pc, there are about 530 stars and only about 179 under precision RV survey, with only 13 of these stars having at least 200 observations. Those numbers translate to a lower limit

for $\eta_\oplus$ of 2/530 times a survey incompleteness factor or 530/13, or about 15%. Conclusions drawn from ever larger local volume-limited samples have diminishing credibility as the survey incompleteness rises dramatically with increasing stellar count with survey volume.

Another unavoidable incompleteness factor involves the random inclinations of exoplanet orbits. Assuming random inclinations, $(1 - \cos 30^\circ)$ or about 13% of the stars in any volume-limited sample would be expected to have orbital inclinations $\leq 30^\circ$ (with respect to the plane of the sky). Were such systems to harbor planets, their observed K values would be at least a factor of 2 less than if edge-on. For example, the K value for GJ 581g is only $1.3\,\mathrm{ms}^{-1}$. An additional factor of 2 decline in K for those 13% of similar stars that are at low inclinations (and also harbor habitable planets) would bring the observable reflex velocity amplitude down to 0.65 ms^{-1}, at or below the expected stellar jitter for the even the quietest stars. With today's largest telescopes and cutting-edge RV precision (1 ms^{-1}), for stars as faint as typical nearby M dwarfs, photon statistics dominate the error budget and, in combination with stellar jitter, make routine and wholesale detectability of such low K values extremely unlikely given the available cadence of the present surveys. We can conservatively expect another factor of at least 13% incompleteness correction in our present surveys of this volume-limited sample.

So, finding a habitable exoplanet system this soon among the nearest few hundreds of stars in the local stellar neighborhood, in spite of the present high level of survey incompleteness and including our own solar system also as a habitable system implies that $\eta_\oplus$ could be on the order of a few tens of percent.

8. Summary

We have presented 11 years of precision HIRES RV data for GJ 581. Our 122 velocities, when combined with the 119 high-quality HARPS velocities of Mayor09 indicate 6 companions in Keplerian motion around this star. The data strongly confirm the 5.37-day planet-b, the 12.9-day planet-c, the 67-day planet-d, and the 3.15-day planet-e candidates previously announced by Bonfils05, Udry07, and Mayor09. The data also indicate two more planets in this system a $7.0\,M_{\oplus}$ 433-day planet and a $3.1\,M_{\oplus}$ 36.6-day planet. The latter orbits squarely in the habitable zone of the star.

The National Academy of Science's recently released 2010 Astronomy and Astrophysics Decadal report lists "seeking nearby habitable planets" as one of its top three objectives for the coming decade. For the past decade, the Doppler velocity method has been the most productive channel for planet detection. In coming years, RV detection will almost certainly continue to delineate the closest and astrobiologically most compelling planets, limited mostly by available telescope time. As the RV amplitudes of truly habitable planets are near the detection limit, collaboration between leading teams would be extremely helpful. The planet candidate GJ 581g presented here, if confirmed, offers a compelling case for a potentially habitable planet, but its RV signature required the combined power of extensive HARPS + HIRES data sets. RV precisions approaching 1 ms^{-1}, and cadences of hundreds of observations on the quietest stars are necessary to securely detect such low-mass planets. GJ 581 does seem to be one of those very quiet stars, with an apparent stellar jitter of no more than 1.4 ms^{-1}. Remarkably, the star has maintained this low level of jitter for 11 years now.

A straightforward and very cost-effective way to realize the 2010 Decadal report's goal of seeking nearby habitable planets, without the need to develop a new generation of "advanced" precision optical or infrared spectrometers, is to build dedicated 6-8 meter class

Automated Planet Finder telescopes, one in each hemisphere. Such dedicated telescopes, instrumented with today's state-of-the-art precision radial velocity spectrometers, like HARPS or HIRES or Magellan's new PFS (Planet Finder Spectrometer) could, within a few short years, provide the necessary cadences of hundreds of observations on all of the nearby quiet G, K, and M dwarf stars within 10 pc, in all probability revealing many other nearby potentially habitable planets. Riding on the coat tails of existing engineering by closely copying the Magellan 6.5-m telescopes, each facility could probably be built (and instrumented with a precision RV spectrometer) for about $50 million, or $100 million total for telescopes in both hemispheres. Indeed, if $\eta_{\oplus}$ is really as high as several tens of percent (or is even only no more than a few percent) having only a single planet finder in one hemisphere could accomplish pretty much the same goal, for a mere $50 million. With this single capital investment, one could make sure, swift, and cost-effective progress on one of the 2010 Decadal report's three primary science goals.

Finally, it is important to keep in mind that, though all 6 planets presented here are well-supported by the calculated reduced chi-squared statistics and also by several different variants of FAP statistics, and the entire 6-planet system is consistent with the combined data set from both teams, caution is warranted as most of the signals are small. And there may yet be unknown systematic errors in either or both data sets. For example, Pont et al. (2010) have recently concluded from a detailed analysis of HARPS CoRoT-7 data that "On the whole, there is a mounting body of evidence that unexplained variations at the 5-10 ms^{-1} level may exist in HARPS RVs for targets in the brightness range of CoRoT-7." GJ 581 is only about a magnitude brighter that CoRoT-7, so it may not be completely out of the question that HARPS data for GJ 581 might also be affected by such unexplained errors. And to be completely fair, the HIRES data set could also have undiscovered systematic errors lurking within. This is very difficult work and there is no shame or dishonor in uncovering residual systematic errors at these levels of precision. Collegial and unabashed

inter-team comparisons on stars like GJ 581 and GJ 876 will be crucial to quantifying the true precision limits of any team's data sets. Finally, because of the very small amplitudes involved, allowing significant eccentricities into the Keplerian fitting tree may yield viable alternate solutions. Here, phase gaps in data sets become problematical as fitting routines generally allow eccentricity to utilize these gaps, driving up the eccentricity artificially to enhance the quality of the fit, and hiding much of the velocity swing from eccentricity in the phase gap. Such situations sometimes result in misleading solutions that can overlook or mask additional planets in the system.

Confirmation by other teams through additional high-precision RVs would be most welcome. But if GJ 581g is confirmed by further RV scrutiny, the mere fact that a habitable planet has been detected this soon, around such a nearby star, suggests that $\eta_{\oplus}$ could well be on the order of a few tens of percent, and thus that either we have just been incredibly lucky in this early detection, or we are truly on the threshold of a second Age of Discovery.

SSV gratefully acknowledges support from NSF grant AST-0307493. RPB gratefully acknowledges support from NASA OSS Grant NNX07AR40G, the NASA Keck PI program, and from the Carnegie Institution of Washington. NH acknowledges support from the NASA Astrobiology Institute under Cooperative Agreement NNA04CC08A at the Institute for Astronomy, University of Hawaii, and NASA EXOB grant NNX09AN05G. GWH and MHW acknowledge support by NASA, NSF, Tennessee State University, and the State of Tennessee through its Centers of Excellence program. The work herein is based on observations obtained at the W. M. Keck Observatory, which is operated jointly by the University of California and the California Institute of Technology, and we thank the UC-Keck and NASA-Keck Time Assignment Committees for their support. We also acknowledge the contributions of fellow members of our previous California-Carnegie Exoplanet team in helping to obtain some of the earlier RVs presented in this paper. We

also wish to extend our special thanks to those of Hawaiian ancestry on whose sacred mountain of Mauna Kea we are privileged to be guests. Without their generous hospitality, the Keck observations presented herein would not have been possible. Finally, SSV would like to extend a very special thanks to his wife Zarmina Dastagir for her patience, encouragement, and wise counsel. And even though, if confirmed, the habitable planet presented herein will officially be referred to by the name GJ 581g, it shall always be known to SSV as "Zarmina's World".

Facilities: Keck.

REFERENCES

Adams, F. C., & Laughlin, G. 2006, ApJ, 649, 992.

Bean, J. L., Benedict, G. F., & Endl, M. 2006, ApJ, 653, L65.

Beust, H., Bonfils, X., Delfosse, X., & Udry, S. 2008, A&A, 479, 277.

Bonfils, X., Forveille, T., Delfosse, X., Udry, S., Mayor, M., Perrier, C., Bouchy, F., Pepe, F., Queloz, D., & Bertaux, J.-L. 2005, A&A, 443, L15.

Butler, R. P., Marcy, G. W., Williams, E., McCarthy, C., Dosanjh, P., & Vogt, S. S. 1996, PASP, 108, 500.

Butler, R.P., Howard, A.W., Vogt, S.S., & Wright, J.T. 2008, ApJ, accepted.

Chabrier, G., & Baraffe, I. 2000, Ann. Rev. Astron. & Astrophys., 38, 337.

Chambers, J. E. 1999, MNRAS, 304, 793.

Chylek, P., & Perez, M. R. 2007, eprint arXiv:0709.1476

Cumming, A. 2004, MNRAS, 354, 1165

Dawson, R.I. & Fabrycky, D.C. 2010, ApJ, submitted.

Delfosse, X. et al. 1998, A&A, 331, 581.

Delfosse, X., Forveille, T., Segransan, D. Beuzit, J.-L., Udry, S., Perrier, C. & Mayor, M. 2000, A&A, 364, 217.

Gilliland, R.L., & Baliunas, S.L. 1987 ApJ, 314, 766.

Hall, J. C., Henry, G. W., Lockwood, G. W., Skiff, B. A., and Saar, S. H. 2009, AJ, 138, 312

Henry, G. W. 1999, PASP, 111, 845

Henry, G. W., Fekel, F. C., & Hall, D. S. 1995, AJ, 110, 2926

Ida, S., & Lin, D. 2005, ApJ, 626, 1045.

Johnson, J., & Apps, K. 2005, ApJ, 699, 933.

Joshi, M. M., Haberle, R. M., and Reynolds, R. T. 1997 Icarus, 129, 450.

Joshi, M. 2003 Astrobiology, 3, 415.

Laskar, J. 1997, A&A, 317, L75.

Laughlin, G., Bodenheimer, P., & Adams, F. C. 2004, ApJ, 612, L73.

Lissauer, J. J., & Rivera, E. J. 2001, ApJ554, 1141.

Lockwood, G. W., Skiff, B. A., Henry, G. W., Henry, S. M., Radick, R. R., Baliunas, S. L., Donahue, R. A., and Soon, W. 2007, ApJS, 171, 260

Jonathan I. Lunine, Debra Fischer, H.B. Hammel, Thomas Henning, Lynne Hillenbrand, James Kasting, Greg Laughlin, Bruce Macintosh, Mark Marley, Gary Melnick, David Monet, Charley Noecker, Stan Peale, Andreas Quirrenbach, Sara Seager, Joshua N. Winn. Astrobiology. October 2008, 8(5): 875-881.

Marcy, G. W., Butler, R. P., Vogt, S. S., Fischer, D. A., Henry, G. W., Laughlin, G., Wright, J. T., & Johnson, J. A., 2005, ApJ, 619, 570.

Mardling, R. A. 2007, MNRAS, 382, 1768.

Mayor, M. et al. 2009, A&A, 507, 487.

Meschiari, S., Wolf, A. S., Rivera, E., Laughlin, G., Vogt, S., & Butler, P. 2009, PASP, 121, 1016

Meschiari, S., & Laughlin, G. P. 2010, ApJ, 718, 543

Murray, C. D., & Dermott, S. F. 1999, Solar System Dynamics (Cambridge: Cambridge Univ. Press).

Nobili, A., & Roxburgh, I. W. 1986, Relativity in Celestial Mechanics and Astrometry. High Precision Dynamical Theories and Observational Verifications, 114, 105.

Paulson, D. B., Saar, S. H., Cochran, W. D., and Henry, G. W. 2004, AJ, 127, 1644

Pont, F., Aigrain, S., and Zucker, S. 2010, MNRAS, (submitted), eprint arXiv:1008.3859

Press, W. H., Teukolsky, S. A., Vetterling, W. T., & Flannery, B. P. 1992, Numerical Recipes: The Art of Scientific Computing (2nd Edition; Cambridge, U.K.: Cambridge University Press).

Queloz, et al. 2001, A&A, 379, 279

Rojas-Ayala, B., Covey, Kevin R., Muirhead, Philip S., and Lloyd, James P. ApJ720, L113.

Schlaufman, K. C., & Laughlin, G. 2010, arXiv:1006.2850

Seager, S., Kuchner, M., Hier-Majumder, C. A., & Militzer, B. 2007, ApJ, 669, 1279.

Selsis, F., Kasting, J. F., Levrard, B., Paillet, J., Ribas, I., & Delfosse, X. 2007, A&A, 476, 1373.

Turnbull, M., & Tarter, J. 2003, ApJS, 149, 423.

Udry, S. et al. 2007, A&A, 469, L43.

Udry, S. et al. 2008, VizieR On-line Data Catalog: J/A+A/469/L43.

Vogt, S. S., Allen, S. L., Bigelow, B. C., Bresee, L., Brown, B., Cantrall, T., Conrad, A., Couture, M., Delaney, C., Epps, H. W., Hilyard, D., Hilyard, D. F., Horn, E., Jern, N., Kanto, D., Keane, M. J., Kibrick, R. I., Lewis, J. W., Osborne, J., Pardeilhan,

G. H., Pfister, T., Ricketts, T., Robinson, L. B., Stover, R. J., Tucker, D., Ward, J., & Wei, M. Z. 1994 SPIE, 2198, 362.

von Bloh, W., Bounama, C., Cuntz, M., & Franck, S. 2007, A&A, 476, 1365.

Weis, E. W. 1994, AJ, 107, 1135

Wright, J. T. 2005, PASP, 117, 657.

This manuscript was prepared with the AAS LaTeX macros v5.2.

Table 1. Radial Velocities for GJ 581

JD (-2450000)	RV (ms^{-1})	error (ms^{-1})
1409.76222	6.96	1.89
1586.14605	-10.24	3.22
1704.91213	0.47	2.89
2003.95507	-4.37	3.65
2100.86678	-19.45	2.22
2161.73096	3.35	2.19
2162.73165	10.73	2.38
2335.15024	6.87	2.33
2487.79326	-7.30	3.77
2712.05433	-10.96	2.10
2828.87708	7.75	2.25
3077.15398	-7.18	3.18
3239.82508	-2.50	2.60
3426.14551	-2.74	4.82
3748.16323	-4.97	1.96
3754.14596	-8.68	1.97
3932.80588	2.40	1.95
3960.83771	12.14	1.90
3961.77279	4.38	1.57
3962.77418	-4.97	2.40

Table 1—Continued

JD (-2450000)	RV (ms^{-1})	error (ms^{-1})
3963.81985	-9.92	1.78
3982.78069	14.04	1.92
4130.14636	-14.79	1.84
4131.16220	-4.58	2.58
4139.16155	1.60	1.92
4246.81907	-4.50	1.18
4247.92767	-9.21	1.84
4248.82815	-7.84	1.48
4249.90281	6.45	1.38
4250.81292	18.17	1.95
4251.81942	7.61	1.30
4255.79771	7.35	3.62
4277.76996	17.11	1.68
4278.78138	14.06	1.71
4279.78247	-10.60	2.03
4285.78969	-15.08	2.54
4294.84381	-0.04	2.04
4300.81847	-0.76	1.83
4304.79872	16.63	2.24
4305.80545	2.61	1.45

Table 1—Continued

JD (-2450000)	RV (ms^{-1})	error (ms^{-1})
4306.83201	-8.05	2.31
4307.83943	-8.03	1.47
4308.82016	1.74	1.27
4309.80568	13.32	1.26
4310.80271	11.19	1.26
4311.79457	-4.40	1.23
4312.79306	-7.14	1.13
4313.80176	8.14	1.45
4314.82230	13.67	1.35
4318.79357	-5.91	1.44
4335.75166	5.83	1.35
4336.78425	14.68	1.84
4339.72676	-8.58	2.69
4343.74861	-0.29	2.06
4345.74397	-5.82	1.94
4461.17458	3.57	2.13
4545.09518	4.98	1.95
4546.07813	17.48	1.52
4547.07715	9.06	2.74
4547.99454	-3.97	2.45

Table 1—Continued

JD (-2450000)	RV (ms^{-1})	error (ms^{-1})
4600.98896	13.54	2.03
4601.90368	-8.33	2.69
4633.86049	-6.47	1.49
4634.86134	-12.30	1.27
4635.87975	-5.69	1.19
4636.88690	12.26	2.07
4637.88502	15.38	1.56
4638.94288	-1.08	1.40
4639.91382	-11.27	1.39
4640.92943	-6.50	1.95
4641.90267	5.64	1.33
4643.88456	0.95	1.74
4666.84246	-7.60	1.25
4667.84194	-8.11	2.07
4671.85435	-9.71	1.33
4672.83453	-3.24	1.00
4673.84973	8.11	1.03
4686.82794	2.60	2.22
4688.77854	-9.57	1.96
4689.77880	3.13	1.29

Table 1—Continued

JD (-2450000)	RV (ms^{-1})	error (ms^{-1})
4701.79211	17.51	1.17
4702.81250	11.35	1.72
4703.80853	-1.73	1.54
4704.80341	-7.99	1.20
4717.72887	14.81	1.48
4718.73784	5.10	2.03
4719.73866	-4.93	1.86
4720.73430	-14.79	1.46
4721.73009	-9.86	1.33
4722.74036	3.80	1.58
4723.73908	6.85	1.62
4903.15067	-14.41	2.08
5021.91811	-10.11	1.43
5022.91286	1.39	1.86
5024.95012	9.32	1.57
5049.86010	4.91	0.90
5050.80706	13.45	0.79
5051.84043	5.28	1.17
5052.86710	-8.12	2.09
5053.79905	-10.89	0.80

Table 1—Continued

JD (-2450000)	RV (ms^{-1})	error (ms^{-1})
5201.15720	16.10	1.58
5202.15734	9.80	1.61
5203.14807	-8.37	1.53
5258.15584	2.44	2.22
5260.13379	16.54	2.11
5338.81312	-4.84	0.53
5338.90357	-3.10	1.59
5338.98795	-1.62	1.33
5339.06181	-1.56	1.82
5340.05371	9.91	1.63
5340.86600	11.62	1.38
5340.95260	9.87	0.58
5341.03351	6.69	0.76
5341.79524	-1.63	0.80
5342.00395	-1.67	0.88
5342.06383	-5.26	1.46
5369.93610	-15.90	1.40
5370.87580	-14.21	1.48
5371.93429	6.73	1.13
5408.89194	-0.40	2.00

Table 1—Continued

JD (-2450000)	RV (ms^{-1})	error (ms^{-1})
5409.76684	15.21	1.48
5409.86682	15.68	1.98

Table 2. Orbital Parameters for GJ 581 Planet Candidates

Planet	Period (days)	K (ms^{-1})	$m \sin i$ ($M_\oplus$)	a (AU)	Mean Anomaly[a] (°)	FAPS
b	5.36841 (0.00026)	12.45 (0.21)	15.6 (0.3)	0.0406163 (1.3e-6)	276.1 (4.9)	6.8e-306
c	12.9191 (0.0058)	3.30 (0.19)	5.6 (0.3)	0.072993 (2.2e-5)	33 (19)	2.3e-33
d	66.87 (0.13)	1.91 (0.22)	5.6 (0.6)	0.21847 (2.8e-4)	56 (27)	2.5e-6
e	3.14867 (0.00039)	1.66 (0.19)	1.7 (0.2)	0.0284533 (2.3e-6)	267 (40)	1.9e-8
f	433 (13)	1.30 (0.22)	7.0 (1.2)	0.758 (0.015)	118 (68)	9.5e-5
g	36.562 (0.052)	1.29 (0.19)	3.1 (0.4)	0.14601 (1.4e-4)	271 (48)	2.7e-6

[a]The fitted mean anomalies are reported at reference epoch JD 2451409.762.

Table 3. Photometric Semiamplitudes Modulo the Radial Velocity Periods

Planet	Planetary Period (days)	Semi-amplitude (mag)
b	5.36841	0.00045 ± 0.00044
c	12.9191	0.00083 ± 0.00044
d	66.87	0.00129 ± 0.00044
e	3.14867	0.00061 ± 0.00045
f	433	...
g	36.562	0.00058 ± 0.00047

Note. — The data set is insufficient to address the 433 day period.